
CAUSAL INFERENCE USING AUGMENTED EPIDEMIC MODELS

A PREPRINT

Heejong Bong
 Department of Statistics
 Purdue University
 West Lafayette, IN 47907
 bong0@purdue.edu

Valérie Ventura **Larry Wasserman**
 Department of Statistics & Data Science
 Carnegie Mellon University
 Pittsburgh, PA 15213
 {vventura, larry}@stat.cmu.edu

January 27, 2026

ABSTRACT

Epidemic models describe the evolution of a communicable disease over time. These models are often modified to include the effects of interventions (control measures) such as vaccination, social distancing, school closings etc. Many such models were proposed during the COVID-19 epidemic. Inevitably these models are used to answer the question: What is the effect of the intervention on the epidemic? These models can either be interpreted as data generating models describing observed random variables or as causal models for counterfactual random variables. These two interpretations are often conflated in the literature. We discuss the difference between these two types of models, and then we discuss how to estimate the parameters of the model. Our focus is causal inference for parameters in epidemic models by adjusting for confounders, allowing time varying interventions.

Keywords G-null paradox, Estimating equations, Marginal structural models

1 Introduction

In this paper we consider the problem of inferring the causal effects of time-varying interventions A_t in epidemics. The term *intervention* can refer to control measures, treatments, public health policies or spontaneous changes in population behavior such as reduced mobility. Such interventions often change over time, often depending on the state of the epidemic. For example, we may want to estimate the effect of vaccinations, masks or social mobility on the number of infections or hospitalizations Y_t over time.

We consider the situation when only one epidemic time series Y_t has been observed, for example, Covid deaths in a single US state. In this case, model free causal effects, such as the difference of mean effects between treated and non-treated groups, cannot be used so some sort of modeling assumption is required. A common approach in causal inference is to assume a *marginal structural model* (MSM, [Robins et al., 2000](#)), which is a type of causal model for time varying inference that describe how the intervention affects the outcome. Furthermore, the assumed MSM is typically simple and easily interpretable. For example, letting $Y_t(a_1, \dots, a_t)$ denote the outcome that would be obtained at time t if the intervention variables A_1, \dots, A_t were set to a_1, \dots, a_t , we might use the model

$$\mathbb{E}[Y_t(a_1, \dots, a_t)] = \beta_0 + \beta_A \sum_{j=1}^t a_j, \quad (1)$$

which says that the expected counterfactual outcome $Y_t(a_1, \dots, a_t)$ at time t is a linear function of the cumulative dose $\sum_{s=1}^t a_s$ up to t . An interesting question is: if an epidemic model is used to describe the data generating process, how can we use it to guide the choice of a MSM?

An example of an epidemic model is the semi-mechanistic model of [Bhatt et al. \(2023\)](#):

$$\begin{aligned}\mathbb{E}[I_t | \bar{A}_t, \bar{I}_{t-1}, \bar{Y}_{t-1}] &= R_t \sum_{s < t} g_{t-s} I_s, \\ \mathbb{E}[Y_t | \bar{A}_t, \bar{I}_t, \bar{Y}_{t-1}] &= \alpha_t \sum_{s < t} \pi_{t-s} I_s,\end{aligned}\tag{2}$$

where I_t are the unobserved infections at t , Y_t are the observed hospitalized, deaths or cases, α_t and R_t are the ascertainment rate and reproduction number, π is the infection to death distribution and g is the generating distribution. To study the effect of an intervention A_t on the epidemic, [Bhatt et al. \(2023\)](#) modeled R_t as

$$R_t \equiv R(\bar{A}_t, \beta) = \frac{K}{1 + \exp(\beta_0 + \beta_A A_t)},\tag{3}$$

where K is the maximum transmission rate. We refer to the model in Eqs. (2) and (3) as *augmented*, since it is extended to incorporate the causal effect of A_t . Other augmented models that have been used in the literature are described in Section 2.

We then face the following questions: how should we interpret an augmented model? How should we estimate the parameters of the model? How should we use the model? Augmented epidemic models have been used both as data generating models (DGMs) and as MSMs. For example, [Bhatt et al. \(2023\)](#) and [Bong et al. \(2024\)](#) produce scenario predictions from the model in Eqs. (2) and (3) – thereby treating it like an MSM – after they fit it to data using the likelihood function in a Bayesian or frequentist framework, respectively – thereby treating it like a DGM. But DGMs and MSMs are, in general, not the same. For example, suppose we observe data (A_t, Y_t) at two time points $t = 1$ and $t = 2$. In the data generating interpretation, the model characterizes the conditional density of the outcome Y_2 , which by the law of total probability can be written as

$$p(y_2 | a_1, a_2) = \int p(y_2 | a_1, y_1, a_2) p(y_1 | a_1) \frac{p(a_2 | a_1, y_1)}{p(a_2 | a_1)} dy_1.\tag{4}$$

In the causal interpretation, the model characterizes the density of the *counterfactual* random variable $Y_2(a_1, a_2)$, which represents the value Y_2 would take if (A_1, A_2) had instead been equal to (a_1, a_2) . As we explain in Section 3, the density of the counterfactual $Y_2(a_1, a_2)$ is

$$p(y_2(a_1, a_2)) = \int p(y_2 | a_1, y_1, a_2) p(y_1 | a_1) dy_1,\tag{5}$$

and we see that $p(y_2 | a_1, a_2) \neq p(y_2(a_1, a_2))$.

The problem with using augmented epidemic models both as DGMs to estimate their parameters, and as MSMs to produce downstream causal inferences such as scenario predictions or estimating causal effects, is that these inferences are inconsistent. We provide three ways to fix this problem (Methods 2, 3 and 4). For completeness, we call Method 1 the approach we described above.

Method 1. The augmented epidemic model is used as a DGM for the observed outcome Y , and its parameters are estimated by maximum likelihood or Bayes. This may seem like the most natural approach but, as we will explain, it should be avoided because it leads to the g -null paradox and yields inconsistent causal estimators. The reason is that, in these models, correlation and causation are entangled and cannot be separated.

Method 2. As in Method 1, the augmented epidemic model is used as a DGM. The causal effect is extracted from the DGM using the g -formula (see Eq. (9)) and the model parameters are then estimated using estimating equations (see Eq. (14)).

Method 3. The augmented epidemic model is used as an MSM, that is as a model for the counterfactual $Y(a)$. The parameters are estimated using estimating equations. Method 3 is the simplest approach and is standard in causal inference.

Method 4. As with Method 3, we use the augmented epidemic model as an MSM for the counterfactual $Y(a)$. Then, in contrast to Method 3, we construct a full DGM in a way that is consistent with the MSM. Then we can apply maximum likelihood to the full model and obtain consistent estimates. In terms of model construction, this is the most technically challenging approach.

Methods 2, 3 and 4 all produce valid downstream causal inference. In our view, Method 3 is the simplest and most natural, and accords with common practice in causal inference. An other advantage of Method 3 is that it handles confounders more easily, because they are added to the propensity score, which is an ingredient in the estimating equations. In contrast, for Methods 1, 2 and 4, confounders must be included in the DGM, which requires more modeling assumptions. Ultimately, we recommend Method 3 but we shall consider all four approaches.

1.1 Related Work

The literature on causal inference is vast. Good references for background include [Hernan and Robins \(2020\)](#); [Imbens and Rubin \(2015\)](#); [Pearl \(2009\)](#). Of particular relevance is [Robins et al. \(2000\)](#) which defines MSMs. We will mainly be concerned with causal inference from a single time series because that's how most epidemic data arise; some of the challenges in such settings have been discussed in [Cai et al. \(2024\)](#).

The literature on epidemic modeling is also very large. However, papers dealing with epidemic models using explicit causal methods are less common. [Halloran and Struchiner \(1995\)](#) deals explicitly with infectious diseases in a causal framework and considers violations of the “no interference” assumption in which one subject’s outcome can be affected by another subject’s intervention. [Bhatt et al. \(2023\)](#); [Flaxman et al. \(2020\)](#) study the effect of various interventions during the Covid pandemic using the semi-mechanistic model in Eqs. (2) and (3). [Bonvini et al. \(2022\)](#) consider the effect of social mobility on deaths for the Covid pandemic. They use the approach described in this paper (Method 3). [Ackley et al. \(2017\)](#) consider how causal graphs might be used in the context of SIR models. [Feng and Bilinski \(2024\)](#) study a particular causal method, known as differences in differences, in the context of SIR models. [Barrero Guevara et al. \(2025\)](#) show how causal structural models can be used to help formulate the study of the causal effects of climate on infectious disease transmission. [Callaway and Li \(2023\)](#) consider multiple time series corresponding to different locations with a binary intervention that occurs at a single time. A SIR model is used to motivate certain assumptions but the method estimates the causal effect by comparing cases in treated locations to the estimated outcome if they had not been treated, using a regression model and propensity weights. The estimator is quite simple and does not rely heavily on the SIR model thanks to the information from multiple locations and the simplicity of the intervention.

Papers that discuss the g -null paradox problem when treating time varying data generating models as MSMs include [Robins \(1986\)](#); [Robins and Wasserman \(1997\)](#); [Bates et al. \(2022\)](#); [Robins \(2000\)](#).

We emphasize that our focus in this paper is on adjustment methods, that is, methods that adjust for observed confounders. There are, of course, other approaches such as differences-in-differences, regression discontinuity designs, instrumental variables, etc.

1.2 Paper Outline

Section 2 presents examples of augmented epidemic models that have been used in the literature. In Section 3 we provide a brief background for causal inference. In Section 4 we explain why the ubiquitous g -null paradox phenomenon arises when Method 1 is used and how Methods 2, 3 and 4, described in Sections 5, 6 and 7, provide remedies to it. Finally, we present examples based on simulated and observational data in Section 8, brush on the problem of model misspecification in Section 9 and conclude in Section 10.

The three main takeaways are: (i) When assessing the effect of interventions in times series, maximum likelihood and Bayes estimates of model parameters are typically inconsistent and subsequent causal effect estimates are inconsistent too. Hence, MLEs and Bayes estimates should not be used. (ii) Three alternative methods could be used instead. One of them, Method 3, is easier to implement because it requires fewer model assumptions. (iii) In the context of Method 3, the epidemic model augmented with interventions provides an interpretable marginal structural model.

1.3 Definitions and Terminology

1.3.1 Augmented Models

Suppose we are given a baseline epidemic model $p(\bar{y}_t; \zeta)$ which correctly describes the joint density of \bar{y}_t in the absence of an intervention. An augmented model is a family of densities $p(\bar{y}_t, \bar{a}_t; \zeta, \beta_A)$ with two properties:

- (1) If $\beta_A = 0$ then $p(\bar{y}_t, \bar{a}_t; \zeta, \beta_A) = p(\bar{y}_t; \zeta)$.
- (2) If $\bar{a}_t = (0, \dots, 0)$ then $p(\bar{y}_t, \bar{a}_t; \zeta, \beta_A) = p(\bar{y}_t; \zeta)$, assuming that $a_t = 0$ corresponds to no intervention.

These conditions imply that when there is no intervention we get back the original model. In particular, under the null hypothesis of no causal effect, we have $\beta_A = 0$ and the model reduces to the baseline epidemic model. We write $\theta = (\zeta, \beta_A)$ in what follows.

1.3.2 Causal Graphs

We will sometimes use directed graphs to illustrate models where arrows denote causal relationships. In Fig. 1, Y_t denotes an observed outcome (such as deaths), A_t denotes the intervention of interest (such as public health policies),

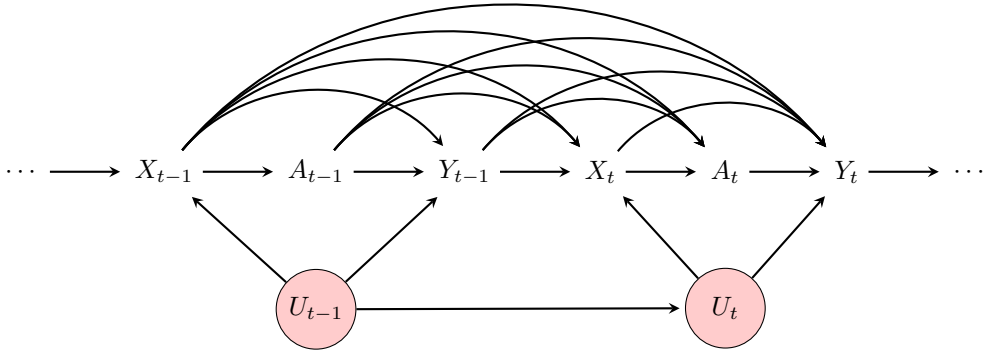


Figure 1: **Example DAG for epidemic data.** The arrows indicate possible causal relationships between the outcome Y , intervention A and confounders X . Latent variables U are in pink; U does not directly affect A – we say that U is a phantom variable. If there were arrows from U to A then U would instead be a confounder.

and X_t denotes confounders. Latent variables are indicated with pink nodes. Importantly, we allow phantom variables U .

1.3.3 Phantom Variables

Phantom variables are unobserved variables that affect Y_t , and possibly all other variables, but that do not directly affect A_t , so they are not confounders. They were initially introduced by [Robins \(1986\)](#) and later named “phantoms” by [Bates et al. \(2022\)](#). They play an important role in causal inference because they are the source of the g -null paradox, as we will explain in Section 4.

Phantoms are ubiquitous. For example, air quality U might affect deaths Y from COVID-19 but will not likely affect mobility A (unless U is extreme). Other factors like healthcare system capacity, pre-existing health conditions, population age distribution, viral strain characteristics, seasonality, socioeconomic status, and public health messaging may influence death rates without directly affecting behaviors such as mobility or mask-wearing. In all these cases, the unobserved variables are not direct causes of treatment, but they shape outcome dynamics and can complicate causal interpretation in time-series settings.

2 Background on Epidemic Models

We review some epidemic models with attention to how interventions have been, or can be, included. In Section 6 we argue that such augmented models can be used as MSMs, which is a type of causal models for time varying inference that describe how the intervention affects the outcome.

Example 1 (SIR Model). *Perhaps the most fundamental epidemic model is the SIR model (Susceptible-Infected-Recovered) due to [Kermack and McKendrick \(1927\)](#). The model is given by three differential equations*

$$\begin{aligned} \frac{dS_t}{dt} &= -\frac{\alpha I_t S_t}{N}, \\ \frac{dI_t}{dt} &= \frac{\alpha I_t S_t}{N} - \gamma I_t, \\ \frac{dR_t}{dt} &= \gamma I_t, \end{aligned} \tag{6}$$

for $t > 0$, where S_t , I_t and R_t are the numbers of susceptibles, infected, and removed (deaths or recovered) at t , $N = S_t + I_t + R_t$ is the total population size, and α and γ are the rates of infection and of removal, respectively. To study the effect of an intervention on the outcome, α could be replaced by $\alpha_t = \alpha e^{\beta_A A_t}$, where β_A is the parameter that modulates the effect of A_t on the subsequent number of infections I_t . Confounders X_t can be added in a similar way, for example, by setting $\alpha_t = \alpha e^{\beta_A A_t + \beta_X^T X_t}$.

[N'konzi et al. \(2022\)](#) include a covariate X_t in a SIR model by modeling the rate of infection as

$$\alpha_t = \frac{\beta_0}{1 + \gamma I X_t},$$

where X_t measures the level of adherence to disease control measures at time t .

[Chernozhukov et al. \(2020\)](#), evaluated the effects of policies on Covid 19 using a system of linear structural equation models which included policies and behaviors. They did not directly use an epidemic model. Rather, they use properties of the SIR model as motivation the form of their model.

Example 2 (Discrete SEIR Model). [Lekone and Finkenstädt \(2006\)](#); [Gibson and Renshaw \(1998\)](#); [Mode and Sleeman \(2000\)](#) proposed a discrete SEIR model which models the numbers of susceptibles S_t , exposed E_t , infected I_t and the cumulative number of removed up to time t , R_t , by

$$\begin{aligned} S_{t+h} &= S_t - B_t, \\ E_{t+h} &= E_t + B_t - C_t, \\ I_{t+h} &= I_t + C_t - D_t, \\ R_{t+h} &= R_t + D_t, \end{aligned} \tag{7}$$

where h represents the time interval (e.g. $h = 1$ day), $B_t \sim \text{Binomial}(S_t, p_{B,t})$ is the number of susceptibles who become infected, $C_t \sim \text{Binomial}(E_t, p_C)$ is the number of new cases and $D_t \sim \text{Binomial}(I_t, p_D)$ is the number of newly removed cases. The parameters are expressed as

$$p_{B,t} = 1 - \exp\left\{-\frac{\eta_t}{N}hI_t\right\}, \quad p_C = 1 - e^{-\rho h}, \quad p_D = 1 - e^{-\gamma h},$$

where η_t is the time-dependent transmission rate, $1/\rho$ is the mean incubation period, $1/\gamma$ is the mean infectious period, and $S_t + E_t + I_t + R_t = N$ is the total population size. Again, we might observe C_t or I_t – the other variables being latent – or we might observe a variable Y_t related to I_t . These papers did not explicitly include interventions but to include an intervention A_t , we could replace η_t with $\eta(\bar{A}_t; \beta) = e^{-\beta_0 - \beta_A A_t}$.

Example 3. [Grigorieva and Khailov \(2015\)](#) use a modified SEIR model

$$\begin{aligned} \dot{S}(t) &= -N^{-1}[u(t)I(t) + v(t)E(t)]S(t) \\ \dot{E}(t) &= N^{-1}[u(t)I(t) + v(t)E(t)]S(t) - \delta E(t) \\ \dot{I}(t) &= \delta E(t) - \gamma I(t) \end{aligned}$$

where $u(t)$ and $v(t)$ model continuous time effects of interventions on infected and on exposed.

Example 4. [Giffin et al. \(2022\)](#) consider a discretized spatial, SIR model

$$\begin{aligned} S_j(t+1) - S_j(t) &= -\lambda_j(t) \\ I_j(t+1) - I_j(t) &= \lambda_j(t) - \gamma I_j(t) \\ R_j(t+1) - R_j(t) &= \gamma I_j(t) \end{aligned}$$

where

$$I_j(t) = \beta_j(t) \frac{S_j(t)}{N} \sum_{k=1}^K W_{jk} I_k(t),$$

W_{jk} is the contact rate between regions j and k and

$$\log \beta_j(t) = \alpha_0 + X_j(t)^T \alpha_1 + A_j(t) \delta$$

where $A_j(t)$ is mobility and are $X(t)$ covariates.

3 Background on Causal Inference

Putting aside epidemic models for a moment, we now review some background on causal inference.

First, consider a single outcome Y and a binary intervention $A \in \{0, 1\}$. The *counterfactual* $Y(a)$ is the value the outcome Y would take if the intervention A were set to a . Thus, we now have four random variables $(A, Y, Y(0), Y(1))$ where $Y(0)$ is the value Y would have if $A = 0$ and $Y(1)$ is the value Y would have if $A = 1$. The counterfactuals $Y(0)$ and $Y(1)$ are linked to the observed data (A, Y) by the equation $Y = Y(A)$. If $A = 1$ then $Y = Y(1)$ but $Y(0)$ is unobserved. If $A = 0$ then $Y = Y(0)$ but $Y(1)$ is unobserved. Many causal questions are quantified by these counterfactuals. For example, $\mathbb{E}[Y(1)] - \mathbb{E}[Y(0)]$ is used to quantify the causal effect of the intervention. It can be shown that if there are no confounding variables — variables that affect both Y and A — then $P(Y \leq y | A = a) = P(Y(a) \leq y)$ so that the distribution of the counterfactual $Y(a)$ is the same as the conditional distribution

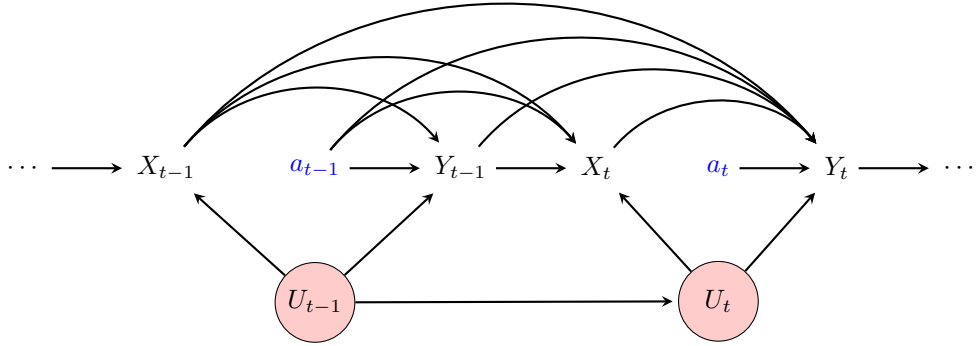


Figure 2: **Intervention graph** from Fig. 1 after setting $\bar{A}_t = \bar{a}_t$.

of the observable Y given A , and thus $\mathbb{E}[Y(a)] = \mathbb{E}[Y|A = a]$. But if there are confounding variables X then $P(Y \leq y|A = a) \neq P(Y(a) \leq y)$ and thus $\mathbb{E}[Y(a)] \neq \mathbb{E}[Y|A = a]$. In this case, it can be shown (under Conditions C1, C2 and C3, described below) that

$$P(Y(a) \leq y) = \int P(Y \leq y|A = a, X = x)dP(x). \quad (8)$$

Thus we can derive the distribution of $Y(a)$ from the distribution for (X, A, Y) using Eq. (8).

Now consider observed time series data of the form

$$(X_1, A_1, Y_1), \dots, (X_T, A_T, Y_T),$$

where A_t is some intervention at time t , Y_t is the outcome of interest at t and X_t refers to potential confounding variables which might affect A_t and Y_t (and future values). As above, the causal effect of the intervention can be quantified by the counterfactual $Y_t(\bar{a}_t)$, which is the value Y_t would have if a hypothetical intervention sequence was $\bar{a}_t = (a_1, \dots, a_t)$ rather than the actual observed sequence $\bar{A}_t = (A_1, \dots, A_t)$. For example, suppose that $a_t = 1$ means that there is a mandate to wear masks and $a_t = 0$ means that there is no mask mandate. Then $Y_t(0, 0, \dots, 0)$ is the outcome at time t if there was never a mask mandate. In some literature, $\mathbb{E}[Y_T|\text{do}(\bar{a}_T)]$ is denoted by $\mathbb{E}[Y_T|\text{do}(\bar{a}_T)]$.

Confounders are generally present in the time series setting because Y_s typically affects future values Y_t and A_t for $t > s$, as depicted in Fig. 1. Then causal and association effects are different, e.g. $\mathbb{E}[Y_t(\bar{a}_t)] \neq \mathbb{E}[Y_t|A_t = \bar{a}_t]$. Robins (1986) proved that

$$\mathbb{E}[Y_t(\bar{a}_t)] = \psi(\bar{a}_t),$$

where

$$\psi(\bar{a}_t) \equiv \int \dots \int \mathbb{E}[Y_t|\bar{x}_t, \bar{y}_{t-1}, \bar{a}_t] \prod_{s=1}^t p(x_s, y_s|\bar{x}_{s-1}, \bar{a}_{s-1}, \bar{y}_{s-1}) dx_s dy_s, \quad (9)$$

provided Conditions (C1)-(C3) below are met. In what follows, we will often write $\psi(\bar{a}_t; \theta)$ where θ denotes any parameters that are involved. Eq. (9) is known as the *g-formula* for the mean causal effect, but there are similar expressions for densities, cdf's, quantiles etc. In particular, let $p_{\bar{a}_t}(y_t)$ denote the density of counterfactual $Y_t(\bar{a}_t)$ evaluated at y_t . Then

$$p_{\bar{a}_t}(y_t) = \int \dots \int p(y_t|\bar{x}_t, \bar{a}_t, \bar{y}_{t-1}) \prod_{s=1}^t p(x_s, y_s|\bar{x}_{s-1}, \bar{a}_{s-1}, \bar{y}_{s-1}) dx_s dy_s, \quad (10)$$

which extends Eq. (8) to the time series setting.

The *g-formula* has a graphical interpretation. Starting with a directed graph G such as Fig. 1, form a new graph G^* in which all arrows pointing into any A_s , $s \leq t$, are removed and in which any A_s is fixed at a value a_s ; see Fig. 2. Eq. (10) is then the marginal density for Y_t corresponding to the density in the graph G^* .

The *g-formula* is valid under three conditions:

(C1) No interference: if $\bar{A}_t = \bar{a}_t$ then $Y_t(\bar{a}_t) = Y_t$.

(C2) Positivity: there exists $\epsilon > 0$ such that $\pi(a_t | \bar{x}_t, \bar{a}_{t-1}, \bar{y}_{t-1}) > \epsilon$ for all values of \bar{x}_t , \bar{a}_t and \bar{y}_{t-1} , where $\pi(a_t | \bar{x}_t, \bar{a}_{t-1}, \bar{y}_{t-1})$ is the density of A_t given the past.

(C3) No unmeasured confounding: the variable $Y_t(\bar{a}_t)$ is independent of A_t given the past measured variables.

Condition (C1) means that the observed Y_t is equal to the counterfactual $Y_t(\bar{a}_t)$ if the observed intervention sequence \bar{A}_t happens to equal \bar{a}_t . This means a subject's outcome is affected by their intervention but not affected by another subject's intervention. This assumption can be violated if there are spillover effects from one subject to another. For example, in the case of vaccines, a subject's outcome (infection) can be affected by the vaccine status of other individuals. The no interference assumption is reasonable when such spillover are considered unlikely. In cases where the outcome is a geographic region (such as a county), no interference is reasonable if the main effect is expected to be local. Condition (C2) means that, conditional on the past, every subject has nonzero probability of receiving intervention at any level. Condition (C3) means that we have measured all important confounding variables, which are variables that affect the intervention and the outcome.

Alternatively, one can specify a simple model for counterfactual $Y_t(\bar{a}_t)$ directly instead of applying the g -formula, akin to specifying a regression model for the effect of \bar{a}_t on Y_t . Eq. (1) provides an example. This is called a *marginal structural model* (MSM; Robins et al., 2000). This approach is semi-parametric, in the sense that we do not need a model for the joint distribution of the time series, $p(y_t | \bar{x}_t, \bar{a}_t, \bar{y}_{t-1})$, since we do not need to apply the g -formula in Eq. (9) or Eq. (10). However, the trade-off for simplicity is that MSMs often fail to incorporate domain-specific knowledge. In contrast, the approach we advocate for in Section 6 (Method 3) includes knowledge about underlying epidemic dynamics by interpreting augmented epidemic models as causal densities $p_{\bar{a}_t}(y_t; \theta)$. That is, we treat augmented epidemic models as MSMs for the counterfactual $Y_t(\bar{a}_t)$.

Next we turn to the problem of parameter estimation.

4 Method 1: Maximum Likelihood Estimation and the Problem of Phantom Bias

Method 1 consists of using maximum likelihood or Bayesian methods to estimate the model parameters (estimates are based on the likelihood function so the model is implicitly thought of as a DGM for Y) then using the fitted model to compute the causal effect of A on Y or make scenario predictions for $Y(a)$ (so the model is now implicitly thought of as a causal model for $Y(a)$). Then we run into a problem first identified by Robins (1986): maximum likelihood and Bayes estimates of causal effects are inconsistent. Robins (1986) called this the *g*-null paradox because the effect is especially pernicious in the null case, when there is no causal effect but the estimated causal effect will be nonzero.

Example 5 (Synthetic example). *To illustrate this, assume that we have data that conforms with the directed graph in Fig. 3, from Robins and Wasserman (1997) Section 1.3. To estimate the causal effect of A_0 or A_1 on Y_1 , suppose that we assume the model*

$$\begin{aligned} A_0 &\sim p(a_0), \\ X_1 &\sim \text{Bernoulli}(\text{expit}(\xi_0 + \xi_1 A_0)), \\ A_1 &\sim p(a_1 | I_1, A_0), \\ Y_1 &= \beta_0 + \beta_1 A_0 + \beta_2 X_1 + \beta_3 A_1 + \delta, \end{aligned}$$

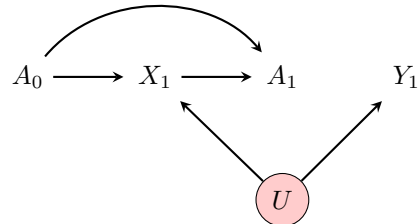


Figure 3: **Effect of phantoms.** The latent phantom variable U is not a confounder because it has no arrows to A_0 or A_1 . Neither A_0 nor A_1 have a causal effect on Y_1 . The variable X_1 is a collider, meaning that two arrowheads point to X_1 . This implies that Y_1 and (A_0, A_1) are dependent conditional on X_1 , which in turn implies that the parameters that relate Y_1 to (A_0, A_1) in the epidemic model will be non-zero even though there is no causal effect.

where δ are mean 0 Normal random variables and p is a logistic model, to which we apply the g -formula to obtain the causal effect on Y_1 of setting (A_0, A_1) to (a_0, a_1) :

$$\psi(a_0, a_1) = \mathbb{E}[Y_1(a_0, a_1)] = \beta_0 + \beta_1 a_0 + \beta_2 \text{expit}(\xi_0 + \xi_1 a_0) + \beta_3 a_1.$$

Note that U did not appear in the model because it is not observed.

The true value of the causal parameter $\beta_A = (\beta_1, \beta_3)$ should be $(0, 0)$ since there is no path from A_0 or A_1 to Y_1 in Fig. 3, and thus no causal effect of (A_0, A_1) on Y_1 . However, [Robins \(1986\)](#); [Robins and Wasserman \(1997\)](#) showed that the maximum likelihood estimators $\hat{\beta}_1$ and $\hat{\beta}_3$ are not zero and in fact converge to nonzero numbers in the large sample limit. Consequently, the estimated causal effect depends on (A_0, A_1) , even though (A_0, A_1) has no effect on Y_1 . This happens because there is a phantom U that affects X_1 and Y_1 , which makes X_1 a collider on the path Y_1, U, X_1, A_0, A_1 and in turn induces conditional dependence between Y_1 and (A_0, A_1) .

Example 6 (Semi-mechanistic Hawkes model). Consider the semi-mechanistic model in Eq. (2), with reproduction number $R(\bar{A}_t, \beta)$ in Eq. (3). If confounders X_t exist, we could include them in $R(\bar{A}_t, \beta)$ by adding the additive term $\beta_X X_t$

$$R(\bar{A}_t, \beta) = \frac{K}{1 + \exp(\beta_0 + \beta_X X_t + \beta_A A_t)}, \quad (11)$$

which is a standard strategy in the regression set-up. The ML estimates of the parameters are not available in closed form but can be obtained numerically ([Bong et al., 2024](#)). The simulation study in Section 8.1 Fig. 5a shows that the ML estimate of the causal effect β_A in Eq. (11) is biased. In particular, when there is no causal effect ($\beta_A = 0$), the ML estimate is significantly different from zero.

In the two examples above, the phantoms create a situation where there is no causal effect, yet the estimated causal effect is nonzero. This happens because sequentially specified non-linear parametric models are not variation independent: causation and conditional dependence between outcome and treatment induced by phantoms are tied together in the parameterization of the model. Essentially, there are not enough parameters to model the two effects separately. Moreover, the ML and Bayes parameter estimates are driven strongly by the conditional dependence rather than by the causal effect. Then both the causal and dependence estimates will be nonzero even though there is no causal effect. To summarize, letting γ represent some measure of conditional dependence and β_A denote the causal parameter, we have

$$\underbrace{\beta_A = 0 \text{ but } \gamma \neq 0}_{\text{due to phantoms}} \implies \underbrace{\hat{\gamma} \neq 0}_{\text{due to estimation based on likelihood}} \implies \underbrace{\hat{\beta}_A \neq 0}_{\text{due to variation dependence}}.$$

That is, the g -null paradox is due to three things: phantoms, which enable conditional dependence between outcome and treatment even though there is no causal effect, variation dependence between causal and dependence effects, and the fact that the causal estimate is nonzero due to dependence.

The fact that in the real world we can have dependence but no causal effect and the model cannot represent this, means that the model is misspecified. If Θ_0 denotes the parameter values that correspond to no causal effect and Θ_+ denotes the parameter values that correspond to conditional dependence, we have that $\Theta_0 \cap \Theta_+ = \emptyset$. This was first pointed out by [Robins \(1986\)](#) and has received much attention since then; see, for example, [Robins and Wasserman \(1997\)](#), [Bates et al. \(2022\)](#), [Robins \(2000\)](#), [Babino et al. \(2019\)](#) and [Evans and Didelez \(2024\)](#). It appears that the problem has gone unnoticed in the literature on modeling epidemics.

The one case where phantoms do not induce a g -null paradox is when all of the equations in the model are linear. This is rarely the case in epidemic models. Generally, any finite dimensional parametric model which models each variable given the past and has some non-linear component and will suffer the g -null paradox. An infinite dimensional (nonparametric) model would solve the problem, but this is not practical when we have many time points due to the curse of dimensionality. This is especially true with a single time series model. There are more complicated parametric models that avoid the problem as we describe in Method 4.

Unlike Method 4, Methods 2 and 3 do not require a more complicated parametric model. They avoid the g -null paradox by estimating the model parameters using estimating equations rather than the likelihood function.

We conclude this section by emphasizing that phantom bias is different than unmeasured confounder bias. Confounders are variables that affect Y_t and A_t . Unobserved confounders render the causal effect unidentifiable. Phantoms do not affect A_t so they do not change the g -formula, and they do not render the causal effect unidentifiable. Rather, they cause the maximum likelihood estimate or Bayes estimate for any sequentially specified non-linear parametric model to be inconsistent.

5 Method 2: Causal Effect Extraction and Estimating Equations

If the epidemic model is treated as a DGM, then we can avoid the g -null paradox by using the following workflow:

- (1) If there are confounders X_t , include them in the DGM.
- (2) Extract the causal effect $\psi(\bar{a}_t; \theta)$ from the DGM using the g -formula in Eq. (9). (Usually, the g -formula is intractable and needs to be computed by simulation.)
- (3) Estimate the parameters of the MSM using estimating equations. Specifically, [Robins et al. \(2000\)](#) showed that θ satisfies

$$\sum_t \mathbb{E} [h_t(\bar{A}_t)(Y_t - \psi(\bar{A}_t; \theta))W_t] = 0 \quad (12)$$

where

$$W_t = \prod_{s=1}^t \frac{\pi(A_s | \bar{A}_{s-1})}{\pi(A_s | \bar{A}_{s-1}, \bar{X}_s, \bar{Y}_{s-1})}. \quad (13)$$

Here, $\pi(A_s | \bar{A}_{s-1}, \bar{X}_s, \bar{Y}_{s-1})$ — called the *propensity score* — is the density of A_s given the whole past and $\pi(A_s | \bar{A}_{s-1})$ is the density of A_s given the past A 's. Both these densities are derived from the DGM. The term $h_t(\bar{A}_t)$ is an arbitrary vector of dimension $\dim(\theta)$ of functions of \bar{A}_t . The simplest choice is $h_t(A_1, \dots, A_t) = 1$ when $\dim(\theta) = 1$. The choice of $h_t(A_1, \dots, A_t)$ affects the variance of the estimator but any choice leads to consistent estimates of θ . In principle, there is an optimal choice that leads to the smallest possible variance but constructing it can be difficult ([Robins, 2000](#); [Kennedy et al., 2015](#)). For simplicity in the three examples of Section 8, we used $h_t(\bar{A}_t) = (1, A_t)$ to estimate the two-dimensional parameters of the MSM.

We define $\hat{\theta}$ to be the solution to the sample version of Eq. (12), namely,

$$\sum_t h_t(\bar{A}_t)(Y_t - \psi(\bar{A}_t; \hat{\theta}))\hat{W}_t = 0 \quad (14)$$

where

$$\hat{W}_t = \prod_{s=1}^t \frac{\hat{\pi}(A_s | \bar{A}_{s-1})}{\hat{\pi}(A_s | \bar{A}_{s-1}, \bar{X}_s, \bar{Y}_{s-1})},$$

with “hats” signifying estimates.

Confidence Intervals. Under some regularity conditions, we have

$$\sqrt{T}(\hat{\theta} - \theta) \rightsquigarrow N(0, \Sigma)$$

with Σ estimated by ([Newey et al., 1987](#))

$$\frac{1}{T} \left[\sum_t \nabla_{\theta} \hat{\phi}_t(\hat{\theta}) \right]^{\top} \left[\sum_{t,s} w(t, s) \cdot \hat{\phi}_t(\hat{\theta}) \hat{\phi}_t(\hat{\theta})^{\top} \right]^{-1} \left[\sum_t \nabla_{\theta} \hat{\phi}_t(\hat{\theta}) \right],$$

where w is a smoothing kernel function and

$$\hat{\phi}_t(\hat{\theta}) \equiv h_t(\bar{A}_t)(Y_t - \psi(\bar{A}_t; \hat{\theta}))W_t,$$

from which we can construct confidence intervals for θ and the causal effect. See also [De Jong \(1997\)](#); [De Jong and Davidson \(2000\)](#); [Andrews \(1991, 1988\)](#) for other estimates of Σ . The conditions needed for the central limit theorem involve mixing conditions which require that correlations in the data eventually die off over time. There is burgeoning research on simulation based inference ([Tomaselli et al., 2025](#)) for situations where asymptotic approximations for confidence intervals are not reliable, although this has yet to be applied to causal inference.

As is evident in Eq. (9), calculating the causal effect $\psi(\bar{A}_t; \theta)$ requires the full joint distribution of $(\bar{X}_t, \bar{A}_t, \bar{Y}_t)$. While possible, postulating a reasonable joint distribution is a daunting task that entails making many assumptions. Additionally, the counterfactual model derived from the DGM is not easily interpretable. Method 3 is related to Method 2, but relies on an easily interpretable counterfactual model and requires fewer distributional assumptions, making Method 3 more practically attractive.

6 Method 3 - Marginal Structural Models and Estimating Equations

In this approach, we do not treat the augmented epidemic model as a DGM and we do not apply steps (1) and (2) of the workflow above. Instead, we interpret the augmented epidemic model as an MSM, that is a model for the counterfactual $Y_t(\bar{a}_t)$. This means that we fix $\bar{A}_t = \bar{a}_t$ and then the model gives the distribution of $Y_t(\bar{a}_t)$. In general, it is unlikely that we will be able to derive a closed form for the distribution of $Y_t(\bar{a}_t)$ because epidemic models are often hierarchical – see, for example, Eqs. (2) and (3) and Section 2 – but we can use Monte Carlo simulation instead. Fix \bar{A}_t at \bar{a}_t , simulate Y_1, \dots, Y_t from the epidemic model parameterized by θ , repeat this simulation N times giving values $Y_1^{(k)}, \dots, Y_t^{(k)}$ for $k = 1, \dots, N$. Then the histogram of $Y_t^{(k)}$, $k = 1, \dots, N$, approximates the distribution of $Y_t(\bar{a}_t)$, and the causal effect – if taken to be the mean of that distribution – is approximated with

$$\psi(\bar{a}_t; \theta) \approx \frac{1}{N} \sum_{k=1}^N Y_t^{(k)}. \quad (15)$$

Having obtained the causal effect $\psi(\bar{a}_t; \theta)$, we now apply the same step (3) of the workflow for Method 2. That is, we estimate θ by solving the estimating equations in Eq. (14) and obtain a confidence interval for θ as specified there. We already discussed the choice of h_t in Eq. (14). As for the propensity score $\pi(A_s | \bar{A}_{s-1}, \bar{X}_s, \bar{Y}_{s-1})$, it is derived from the full joint distribution of $(\bar{X}_t, \bar{A}_t, \bar{Y}_t)$ when we use Method 2, but we must specify a model for it here since we do not assume a model for the full joint distribution.

6.1 Propensity Score Model

When A_t is continuous, a natural choice is an autoregressive model of order k

$$A_t = \chi_0 + \chi_1 A_{t-1} + \dots + \chi_k A_{t-k} + \gamma_0^T X_t + \dots + \gamma_k^T X_{t-k} + \lambda_1 Y_{t-1} + \dots + \lambda_k Y_{t-k} + \epsilon_t$$

where $\epsilon_1, \dots, \epsilon_T \sim N(0, \sigma^2)$. When A_t is binary, a tractable model for the propensity score is the logistic autoregression given by

$$\pi(A_t | \bar{A}_{t-1}, \bar{X}_t) = \pi_t^{A_t} (1 - \pi_t)^{1 - A_t}$$

where

$$\text{logit}(\pi_t) = \chi_0 + \chi_1 A_{t-1} + \dots + \chi_k A_{t-k} + \gamma_0^T X_t + \dots + \gamma_k^T X_{t-k} + \lambda_1 Y_{t-1} + \dots + \lambda_k Y_{t-k}.$$

The parameters can be estimated by maximum likelihood, and the maximum lag k can be estimated using criteria like AIC or BIC.

A challenge is that the estimated propensity score $\widehat{\pi}(A_s | \bar{A}_{s-1}, \bar{X}_s, \bar{Y}_{s-1})$ can sometimes get very small, which causes \widehat{W}_t and the resulting causal estimates to have large variances. Small propensity scores are often a problem in causal inference and these problems are exacerbated in time series models since we have to multiply many weights together in Eq. (13). Dealing with small propensity scores in causal inference is an active area of research. One possibility is to use a method called residual balancing (Zhou and Wodtke, 2020) rather than estimating the propensity score. This method uses moment conditions to estimate the weights W_t directly and leads to more stable estimates. The method was used successfully in Bonvini et al. (2021). For a review on propensity scores see Pan and Bai (2018).

6.2 Challenges for Short Time Series

Estimating the propensity score from a single time series is challenging. All of the above assumes that we have enough observations T to estimate the parameters well. The autoregressive model for the propensity score might have to allow the maximum lag k to be large if interventions in the far past effect current treatment. Estimating the parameters in that case requires a long observation window. Furthermore, the confidence intervals depend on asymptotic Normality which also requires T to be large. If T is not large then we may not be able to estimate the parameters and asymptotic Normality may fail. In these cases, causal inference might be infeasible. If there are multiple time series then the situation might be better. For example, suppose we have a time series for every county in the USA. Then, estimation and inference become feasible again since we have much more information. However, in this case, one might want to allow the parameters to vary across counties which suggests using a hierarchical model. Causal inference with hierarchical models has been studied; see, for example, Feller and Gelman (2015) and Weinstein and Blei (2024). One possibility to estimate the parameters separately for each county, shrink the estimates towards each other then form debiased confidence intervals as in Armstrong et al. (2022); Bong et al. (2024).

6.3 Examples

We finish Section 6 with a rare example for which the causal effect $\psi(\bar{a}_t, \theta)$, if taken to be the mean of the causal distribution, can be computed in closed form instead of approximated by Monte Carlo, as in (15). For this example we also provide the derivatives of the estimating equations in Eq. (14), which are needed to obtain $\hat{\theta}$ numerically. We will use this example in Section 8.1 to illustrate phantom bias.

We also consider the SEIR model, which does not admit a closed form solution for $\psi(\bar{a}_t, \theta)$ and must be approximated by Monte Carlo in (15). We provide Monte Carlo derivatives of this approximation, so that we can use this model to further illustrate phantom bias in Section 8.2.

Example 7 (Semi-mechanistic Model). *Consider the model in Eq. (2), with reproduction number in Eq. (3). A different version takes*

$$\begin{aligned}\mathbb{E}[I_t | \bar{A}_t, \bar{I}_{t-1}, \bar{Y}_{t-1}] &= \sum_{s < t} e^{\beta_0 + \beta_A A_s} g_{t-s} I_s, \\ \mathbb{E}[Y_t | \bar{A}_t, \bar{I}_t, \bar{Y}_{t-1}] &= \alpha_t \sum_{s < t} \pi_{t-s} I_s.\end{aligned}\tag{16}$$

We call Eqs. (2) and (3) the multiplicative version of the semi-mechanistic model and Eq. (16) the exponential version. Notice that for fixed values of \bar{A}_t , α_t , g and π , this model is a set of linear equations and is an example of what is known in the causality world as a linear structural equation model (SEM), for which tricks exist to derive the g -formula in closed-form.

Meaningful dynamics in this model requires some positive infections I_t prior to time $t = 1$. Bhatt et al. (2023) assumed $I_t = 0$ for $t \leq -T_0$ and $I_t = e^\mu$ for $t = -T_0 + 1, \dots, 0$, where μ is a parameter to be estimated and $T_0 = 6$. Let $\bar{I}_0 \equiv (I_{-T_0+1}, \dots, I_0)$ indicate those seeding values in the infection process. (We still exclude those seeding values in the definition of $\bar{I}_t = (I_1, \dots, I_t)$.)

For the exponential model define

$$\Lambda^e = \begin{pmatrix} 0 & 0 & \cdots & 0 \\ g_1 e^{\beta_0 + \beta_A a_1} & 0 & \cdots & 0 \\ g_2 e^{\beta_0 + \beta_A a_1} & g_1 e^{\beta_0 + \beta_A a_2} & \cdots & 0 \\ \vdots & \vdots & \vdots & \vdots \\ g_{t-1} e^{\beta_0 + \beta_A a_1} & g_{t-2} e^{\beta_0 + \beta_A a_2} & \cdots & 0 \end{pmatrix}, \quad \Lambda_0^e = \begin{pmatrix} g_{T_0} e^{\beta_0 + \beta_A a_{-T_0+1}} & \cdots & g_1 e^{\beta_0 + \beta_A a_0} \\ g_{T_0+1} e^{\beta_0 + \beta_A a_{-T_0+1}} & \cdots & g_2 e^{\beta_0 + \beta_A a_0} \\ g_{T_0+2} e^{\beta_0 + \beta_A a_{-T_0+1}} & \cdots & g_3 e^{\beta_0 + \beta_A a_0} \\ \vdots & \vdots & \vdots \\ g_{T_0+t-1} e^{\beta_0 + \beta_A a_{-T_0+1}} & \cdots & g_t e^{\beta_0 + \beta_A a_0} \end{pmatrix},$$

and for the multiplicative model define

$$\Lambda^m = \begin{pmatrix} 0 & 0 & \cdots & 0 \\ g_1 R(\bar{a}_2, \beta) & 0 & \cdots & 0 \\ g_2 R(\bar{a}_3, \beta) & g_1 R(\bar{a}_3, \beta) & \cdots & 0 \\ \vdots & \vdots & \vdots & \vdots \\ g_{t-1} R(\bar{a}_t, \beta) & g_{t-2} R(\bar{a}_t, \beta) & \cdots & 0 \end{pmatrix}, \quad \Lambda_0^m = \begin{pmatrix} g_{T_0} R(\bar{a}_1, \beta) & \cdots & g_1 R(\bar{a}_1, \beta) \\ g_{T_0+1} R(\bar{a}_2, \beta) & \cdots & g_2 R(\bar{a}_2, \beta) \\ g_{T_0+2} R(\bar{a}_3, \beta) & \cdots & g_3 R(\bar{a}_3, \beta) \\ \vdots & \vdots & \vdots \\ g_{T_0+t-1} R(\bar{a}_t, \beta) & \cdots & g_t R(\bar{a}_t, \beta) \end{pmatrix}.$$

Finally, define

$$\Pi = \begin{pmatrix} 0 & 0 & \cdots & 0 \\ \pi_1 \alpha_2 & 0 & \cdots & 0 \\ \pi_2 \alpha_3 & \pi_1 \alpha_3 & \cdots & 0 \\ \vdots & \vdots & \vdots & \vdots \\ \pi_{t-1} \alpha_t & \pi_{t-2} \alpha_t & \cdots & 0 \end{pmatrix}, \quad \Pi_0 = \begin{pmatrix} \pi_{T_0} \alpha_1 & \cdots & \pi_1 \alpha_1 \\ \pi_{T_0+1} \alpha_2 & \cdots & \pi_2 \alpha_2 \\ \pi_{T_0+2} \alpha_3 & \cdots & \pi_3 \alpha_3 \\ \vdots & \vdots & \vdots \\ \pi_{T_0+t-1} \alpha_t & \cdots & \pi_t \alpha_t \end{pmatrix}.$$

Then the marginal structural model $\psi(\bar{a}_t; \theta)$ is given in a closed form as follows.

Theorem 8. For the exponential model,

$$\mathbb{E}[I_t(\bar{a}_t)] = [(id - \Lambda^e)^{-1} \Lambda_0^e \bar{I}_0]_t \tag{17}$$

and

$$\psi(\bar{a}_t; \theta) \equiv \mathbb{E}[Y_t(\bar{a}_t)] = [\{\Pi(id - \Lambda^e)^{-1} \Lambda_0^e + \Pi_0\} \bar{I}_0]_t, \tag{18}$$

where the subscript t represents the t -th element of the outcome vector. For the multiplicative model, the expressions are the same except that Λ^m and Λ_0^m replace Λ^e and Λ_0^e .

Proof. Consider the intervened graph in Fig. 2 with \bar{A}_t set to \bar{a}_t . For this graph, we have

$$\bar{I}_t(\bar{a}_t) = \Lambda^e \bar{I}_t(\bar{a}_t) + \Lambda_0^e \bar{I}_0 + \epsilon,$$

for the exponential model (Eq. (16)), which, as mentioned above, is a linear structural equation model. Now

$$\bar{I}_t(\bar{a}_t) = (id - \Lambda^e)^{-1} \Lambda_0^e \bar{I}_0 + (id - \Lambda^e)^{-1} \epsilon$$

and hence, the last element of this vector is

$$\mathbb{E}[I_t(\bar{a}_t)] = [(id - \Lambda^e)^{-1} \Lambda_0^e \bar{I}_0]_t.$$

Subsequently,

$$\mathbb{E}[\bar{Y}_t(\bar{a}_t)] = \Pi \mathbb{E}[\bar{I}_t(\bar{a}_t)] + \Pi_0 \bar{I}_0 = [\{\Pi(id - \Lambda^e)^{-1} \Lambda_0^e + \Pi_0\} \bar{I}_0]_t.$$

The proof proceeds similarly for the multiplicative model (Eq. (2)), but with Λ^m and Λ_0^m in place of Λ^e and Λ_0^e . \square

Most often, we cannot solve the estimating equations (Eq. (14)) in closed form. In that case, we apply Newton's method, which requires the computation of the first derivative on the left-hand side of the equation with respect to the parameter of interest. Specifically, since β is the key parameter in both the semi-mechanistic model (Eq. (2)) and the SEIR model (Eq. (7)), we provide detailed calculations for the derivative with respect to β .

Example 9 (Semi-mechanistic Model). In Example 7, we derived the closed-form expression for the causal mean $\psi(\bar{a}_t; \theta)$ in a multiplicative semi-mechanistic model as:

$$\psi(\bar{a}_t; \theta) = [\{\Pi(id - \Lambda^m)^{-1} \Lambda_0^m + \Pi_0\} \bar{I}_0]_t.$$

For each component of β (β_0 and β_A), the first derivative of Λ^m with respect to β_i is given by:

$$\frac{\partial}{\partial \beta_i} \Lambda^m(t, s) = g_{t-s} \frac{\partial}{\partial \beta_i} R(\bar{a}_t, \beta) \mathbf{1}\{t > s\},$$

where $\Lambda^m(t, s)$ is parameterized by the rate function $R(\bar{a}_t, \beta)$, and $\mathbf{1}\{t > s\}$ is an indicator function. Similarly, the derivative of Λ_0^m with respect to β_i follows the same structure.

Using the identity from matrix calculus, $\frac{\partial U^{-1}}{\partial x} = -U^{-1} \frac{\partial U}{\partial x} U^{-1}$, we can express the derivative of $\psi(\bar{a}_t; \theta)$ with respect to β_i as:

$$\begin{aligned} \frac{\partial}{\partial \beta_i} \psi(\bar{a}_t; \theta) &= \left[\left\{ \Pi(id - \Lambda^m)^{-1} \frac{\partial \Lambda^m}{\partial \beta_i} (id - \Lambda^m)^{-1} \Lambda_0^m + \Pi(id - \Lambda^m)^{-1} \frac{\partial \Lambda_0^m}{\partial \beta_i} \right\} \bar{I}_0 \right]_t \\ &= \left[\Pi(id - \Lambda^m)^{-1} \left\{ \frac{\partial \Lambda^m}{\partial \beta_i} \mathbb{E}[\bar{I}_t(\bar{a}_t)] + \frac{\partial \Lambda_0^m}{\partial \beta_i} \bar{I}_0 \right\} \right]_t. \end{aligned}$$

The derivative for the exponential model is given similarly.

Example 10 (SEIR Model). The SEIR model in Eq. (7) does not admit a closed-form expression for the causal effect $\psi(\bar{a}_t; \theta)$. In Eq. (15), we proposed estimating this quantity through Monte Carlo approximation. Here, we describe how the derivative of this approximation can also be computed using Monte Carlo samples. First, applying the law of total probability,

$$\begin{aligned} \mathbb{E}_\theta[Y_t(\bar{a}_t)] &= \int \cdots \int \mathbb{E}[Y_t | \bar{B}_{t-1}, \bar{C}_{t-1}, \bar{Y}_{t-1}] \prod_{s=1}^{t-1} dP_{Y_s}(Y_s | \bar{B}_{s-1}, \bar{C}_{s-1}, \bar{Y}_{s-1}) \\ &\quad \times dP_{C_s}(C_s | \bar{B}_{s-1}, \bar{C}_{s-1}, \bar{Y}_{s-1}) \times dP_{B_s|\beta}(B_s | \bar{B}_{s-1}, \bar{C}_{s-1}, \bar{Y}_{s-1}), \end{aligned}$$

where P_{Y_s} , P_{C_s} , and P_{B_s} are binomial distributions. (Note that \bar{a}_s is implicit in some expressions on the right hand side.) The “number of trials” parameters for these variables depend on the conditioning terms \bar{B}_{s-1} , \bar{C}_{s-1} , and \bar{Y}_{s-1} , with success probabilities denoted by p_Y , p_C , and p_B , respectively. Importantly, only $p_{B_s|\beta}$, and consequently $P_{B_s|\beta}$, are parametrized by β through $\eta(\bar{a}_s; \beta)$. Now, suppose we have Monte Carlo samples $\{(\bar{B}_T^{(k)}, \bar{C}_T^{(k)}, \bar{Y}_T^{(k)}) : k = 1, \dots, N\}$ drawn under a given β . For any alternative parameter β' , we approximate the mean using importance sampling as follows:

$$\psi(\bar{a}_t; \theta') \approx \frac{1}{N} \sum_{k=1}^N \mathbb{E}[Y_t^{(k)} | \bar{B}_{t-1}^{(k)}, \bar{C}_{t-1}^{(k)}, \bar{Y}_{t-1}^{(k)}] \prod_{s=1}^{t-1} \frac{dP_{B_s|\beta'}}{dP_{B_s|\beta}}(B_s | \bar{B}_{s-1}^{(k)}, \bar{C}_{s-1}^{(k)}, \bar{Y}_{s-1}^{(k)}),$$

where θ' is θ with component β replaced by β' , and $\frac{dP_{B_s|\beta'}}{dP_{B_s|\beta}}$ is the Radon–Nikodym derivative. Note that when $\beta' = \beta$, the importance sampling estimator reduces to the Monte Carlo approximation for $\psi(\bar{a}_t; \theta)$ as given in Eq. (15).

Next, to compute the derivative of $\psi(\bar{a}_t; \theta)$ with respect to β , we recognize that the derivative of the Radon–Nikodym derivative $\frac{dP_{B_s|\beta'}}{dP_{B_s|\beta}}$ at $\beta' = \beta$ is the gradient of the log-likelihood: $\nabla_\beta \log\{f_{B_s|\beta}(B_s | \bar{B}_{s-1}^{(k)}, \bar{C}_{s-1}^{(k)}, \bar{Y}_{s-1}^{(k)})\}$. By applying the chain rule, we obtain:

$$\nabla_\beta \psi(\bar{a}_t; \theta) \approx \frac{1}{N} \sum_{k=1}^N \mathbb{E}[Y_t^{(k)} | \bar{B}_{t-1}^{(k)}, \bar{C}_{t-1}^{(k)}, \bar{Y}_{t-1}^{(k)}] \sum_{s=1}^{t-1} \nabla_\beta \log\{f_{B_s|\beta}(B_s | \bar{B}_{s-1}^{(k)}, \bar{C}_{s-1}^{(k)}, \bar{Y}_{s-1}^{(k)})\}.$$

7 Method 4 - Causal Preserving Data Generating Models

Method 3 requires two models: an MSM for $Y_t(\bar{a}_t)$ and a model for the propensity score. It does not require a model for the joint distribution $p(\bar{x}_t, \bar{a}_t, \bar{y}_t)$ of the observables. Method 4 consists of constructing a model for $p(\bar{x}_t, \bar{a}_t, \bar{y}_t)$ that preserves the specified epidemic MSM for $Y_t(\bar{a}_t)$. Then we can use maximum likelihood to estimate all the parameters of the model, including the parameters of the causal model. We use the approach developed in [Evans and Didelez \(2024\)](#) based on copulas, which they call a *frugal parameterization*. This requires more modeling than the estimating equation approach but it also avoids the null paradox and has the advantage that one avoids dividing by the propensity score in Eq. (13), which can lead to unstable inference. We will assume throughout this section that all the variables are continuous.

First, we recall some basics about copulas ([Joe, 2014](#)). A copula $C(u_1, \dots, u_d)$ is a joint distribution on $[0, 1]^d$ with uniform marginals. We let $c(u_1, \dots, u_d)$ denote the corresponding density function. A key fact is that any joint density $p(x_1, \dots, x_d)$ for random variables X_1, \dots, X_d can be written as

$$p(x_1, \dots, x_d) = c(F_1(x_1), \dots, F_d(x_d)) \prod_j p_j(x_j) \quad (19)$$

for some copula c , where p_j is the marginal density of X_j and F_j is the corresponding cdf. Thus, copulas provide a way to paste together a set of marginal distributions to form a joint distribution.

One can consider parametric families of copulas $c(u; \theta)$. For example, the Gaussian copula has density

$$c(u) = |\theta|^{-1/2} \exp\left(-\frac{1}{2}\Phi^{-1}(u)^T(\theta - I)\Phi^{-1}(u)\right)$$

where θ denotes a correlation matrix, $\Phi(u) = (\Phi(u_1), \dots, \Phi(u_d))$ and Φ is the standard Normal cdf. The process of constructing parametric families of copulas has a rich literature.

To see how this helps build causal models, first consider observations at a single time point: a vector of confounders $X \in \mathbb{R}^d$, an intervention $A \in \mathbb{R}$, and an outcome $Y \in \mathbb{R}$. Let $p_a(y)$ be the density of a given marginal structural model for the counterfactual $Y(a)$, and let $F_a(y) = \int_{-\infty}^y p_a(s)ds$ denote the cdf. We aim to construct a joint density $p(x, a, y)$ for the observed variables (X, A, Y) that is consistent with the given counterfactual distribution $p_a(y)$. Consistency here means that applying the *g*-formula, i.e., $\int p(y|x, a)p(x)dx$, to the joint density $p(x, a, y)$ recovers the original counterfactual density $p_a(y)$. Under Conditions (C1), (C2) and (C3), we can construct such joint distributions by

$$p(x, a, y) = p_a(x, a, y) = p_a(y)p(a)p_j(x_1) \cdots p_d(x_d)c(F_a(y), G_1(x_1), \dots, G_d(x_d), Q(a)).$$

using Eq. (19), where $p_a(x, a, y)$ denotes the joint density of $(X, A, Y(a))$, and G_j and Q are the cdfs of X_j and A , respectively. We can add parameters to these distributions to define a parametric family

$$\begin{aligned} p(x, a, y; \beta, \gamma, \theta) &= p_a(y; \beta)p(a; \delta) \prod_j p_j(x_j; \gamma_j) \\ &\quad \times c(F_a(y; \beta), G_1(x_1; \gamma_1), \dots, G_d(x_d; \gamma_d), Q(a; \delta); \theta). \end{aligned}$$

Because β and θ parametrize the causation by A and other indirect correlation between A and Y separately, these models are variation independent and avoid the *g*-null paradox ([Evans and Didelez, 2024](#)).

Turning to the time varying case, a similar construction can be used but is much more involved. The recent paper by [Lin et al. \(2025\)](#) shows how to use a class of copulas known as pair copulas to parameterize the joint distribution. The details are fairly involved and we refer the reader to [Lin et al. \(2025\)](#) for details.

The estimating equation approach (Method 3) requires two models: the epidemic MSM and a model for the propensity score. The fully specified, frugal approach (Method 4) requires, in addition, a model for X and a copula. A full exploration of how to construct these models will be quite complicated and we leave this for future work. The advantage of Method 3 is thus that it requires less modeling. The advantage of Method 4 is that we never need to divide by the propensity score which can lead to instability. Also, a fully specified joint distribution (Method 4) may be useful for purposes of interpretability and model checking.

8 Examples

Our first two examples use simulated data to illustrate that phantom variables can induce bias in ML parameter estimates, and that using estimating equations yields unbiased estimates. The last example is an analysis of the effect of a mobility measure – the proportion of full-time work – on COVID-19 deaths in 30 US states at the start of the pandemic. The code vignettes used to generate the results are provided in github.com/Hee jongBong/causepid.

8.1 Semi-mechanistic model simulated data

A time series consistent with the DAG in Fig. 1 is simulated from the semi-mechanistic model in Eq. (2) as follows.

- Seed the infection time series by setting $I_t = 0$ for $t \leq -40$ and $I_t = e^\mu$, $\mu = \log(100)$, for $t = -39, \dots, 0$. The $t = -40$ time cutoff point corresponds to the main support of the generating distribution g used in [Bhatt et al. \(2023\)](#); [Bong et al. \(2024\)](#) and shown in Fig. 4. (More realistic infection data could be simulated from the data generating process described below starting at $t = -39$, but then it is difficult to obtain ML estimates. Details are in [Bong et al. \(2024\)](#).)
- Seed the confounder, intervention and outcome at $t = 0$ with $X_0 = A_0 = 0$ and $Y_0 = I_{-1}$.
- Simulate phantom variables U_t from a Gaussian random process with mean zero and covariance kernel $\Sigma(t, s) = \phi^{|t-s|}$, with $\phi = 0.95$.

Then for $t = 1, \dots, 120$,

1. sample confounders X_t from a Gaussian distribution with mean $\xi_U U_t + \xi_X X_{t-1} + \xi_A A_{t-1} + \xi_Y Y_{t-1}$, with $(\xi_U, \xi_X, \xi_A, \xi_Y) = (0.2, 0, 1, 0)$ and variance $\sigma^2 = 0.09$;
2. generate binary interventions A_t from a Bernoulli distribution with probability

$$\mathbb{P}(A_t = 1 \mid \bar{X}_t, \bar{A}_{t-1}, \bar{Y}_{t-1}) = \frac{e^{\gamma_1 + \gamma_X X_t + \gamma_A A_{t-1} + \gamma_Y Y_{t-1}}}{1 + e^{\gamma_1 + \gamma_X X_t + \gamma_A A_{t-1} + \gamma_Y Y_{t-1}}},$$

where $(\gamma_1, \gamma_X, \gamma_A, \gamma_Y) = (-2.5, 0, 4, 0.001)$;

3. simulate an infection process I_t from a negative binomial distribution with “number of successes” parameter $\nu = 10$ and mean parameter specified in Eq. (2), where g is the generating distribution in Fig. 4, the reproduction number is

$$R(\bar{A}_t, \beta) = \frac{K}{1 + \exp(\beta_0 + \beta_U U_t + \beta_X X_t + \beta_A A_t)}, \quad (20)$$

$K = 6.5$ is the maximum transmission rate, and $(\beta_U, \beta_X) = (0.3, 0)$. We will vary the values of β_0 and β_A , as described below.

Notice that we set $\gamma_X = \beta_X = 0$, meaning that there is no unobserved confounding, to highlight that phantom bias is different than unobserved confounder bias.

4. Finally, simulate an observed time series Y_t – e.g. cases or deaths – according to Eq. (2) with $\alpha_t = 1$ and $\pi_t = \mathbf{1}\{t = 1\}$, for simplicity, so that $Y_t = \mathbb{E}[Y_t \mid \bar{I}_{t-1}, \bar{Y}_{t-1}, \bar{A}_t] \equiv I_{t-1}$ for all t .

The simulation was performed for 21 linearly spaced values of β_A in $[-1, 0]$, and for each value of β_A we let β_0 depend on β_A according to $\beta_0 = -\log(5.5) + 0.5 - \beta_A/2$, to prevent $R(\bar{A}_t, \beta)$ from getting too small or too large, so that the simulated epidemic curves do not explode or plunge to zero. Our parameter choices mostly produced epidemic curves with shapes we typically observe in practice, that is rise, plateau and then slowly decrease. For each β_A , we simulated 200 time series \bar{Y}_t , $t = 1, \dots, 120$, and for each time series, we obtained the ML estimates of $(\beta_0, \beta_A, \beta_X)$ and the seeding parameter μ (this is Method 1) using the package `freqepid` ([Bong et al., 2024](#)), assuming the same DGM we used to simulate the data but for one detail: we assumed reproduction number $R(\bar{A}_t, \beta) = \frac{K}{1 + \exp(\beta_0 + \beta_X X_t + \beta_A A_t)}$ (Eq. (11)) instead of Eq. (20), which was used to simulate the data, since the U_t are not observed. All other parameters were assumed to be known.

Fig. 5a shows the averages of the 200 MLEs of β_A plotted against the true β_A , along with 95% confidence intervals. There is phantom bias. There was no bias when we reproduced the simulation with $\beta_U = 0$ in Eq. (20), confirming that what we see in Fig. 5a is due to phantom variables; see Fig. A.1.

For each simulated time series we estimated (β_0, β_A) per Method 3, by solving the estimating equations in Eq. (14), assuming the MSM in Eq. (2) with reproduction number in Eq. (3), that is $R(\bar{A}_t, \beta) = \frac{K}{1 + \exp(\beta_0 + \beta_A A_t)}$. (Note that

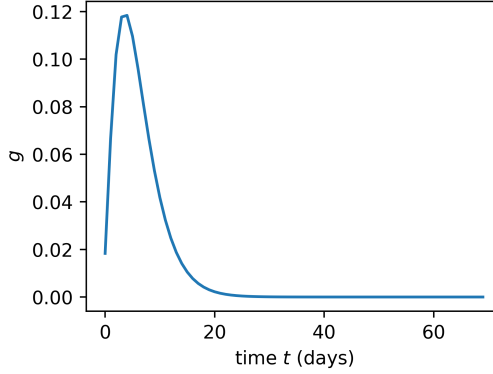
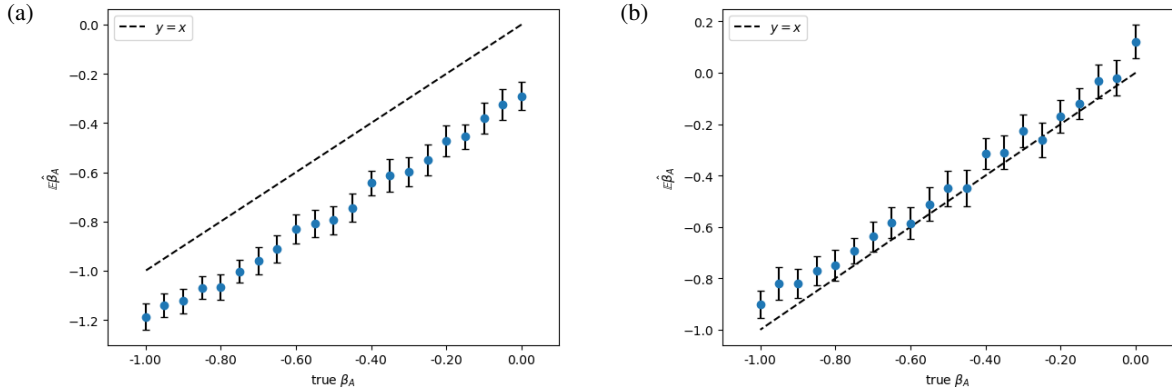
Figure 4: Generating distribution g from Bhatt et al. (2023).

Figure 5: **Causal parameter estimation for semi-mechanistic epidemic model data.** (a) Method 1: ML estimate and (b) Method 3: estimating equations estimate of β_A averaged across 200 repeat simulations (blue dots) with 95%-confidence intervals (error bars), for a range of true β_A values. There is phantom bias in (a) but not in (b). Small biases persist in (b), as evidenced by the confidence intervals excluding the true value of β_A more often than they should. This is due to model misspecification, which we discuss in Section 9.

Eq. (3) depends only on A_t .) We proceeded numerically via Newton's method initialized at the MLEs, and causal effect $\psi(\bar{a}_t, \theta)$ and derivative $\nabla_\beta \psi(\bar{a}_t, \theta)$ obtained following Examples 7 and 9. In Eq. (14), we took $h_t(\bar{A}_t) = (1, A_t)$ and we modeled the denominator of the propensity score W_t (Eq. (13)) using a logistic regression with linear AR(1) logit link,

$$\text{logit}(\pi_t) = \chi_0 + \chi_1 A_{t-1} + \gamma_0 X_t + \lambda_1 Y_{t-1},$$

as described in Section 6.1, and estimated the parameters by maximum likelihood. We proceeded similarly with a logistic AR(1) model for the numerator.

Fig. 5b shows the averages over the 200 simulations of the estimating equation estimates of β_A for each true value of β_A , along 95% confidence intervals. We no longer have phantom bias. Notice that small biases still persist, as evidenced by the confidence intervals excluding the true value of β_A more often than they should. This is due to model misspecification, which we discuss in Section 9.

8.2 SEIR model simulated data

We further illustrate phantom bias using the SEIR model in Example 2. One time series is generated as follows.

- Set $I_0 = 100$, $E_0 = 0$ and $S_0 = N - I_0 - E_0$, with total population $N = 100,000$.
- Simulate phantom variables U_t from a Gaussian random process with mean zero and covariance kernel $\Sigma(t, s) = \phi^{|t-s|}$, with $\phi = 0.95$.

Then for $t = 1, \dots, 120$,

1. sample confounders X_t from a Gaussian distribution with mean $\xi_U U_t + \xi_X X_{t-1} + \xi_A A_{t-1} + \xi_Y Y_{t-1}$, where $(\xi_U, \xi_X, \xi_A, \xi_Y) = (0.5, 0, 1, 0)$ and variance $\sigma^2 = 0.09$.
2. Generate binary interventions A_t from a Bernoulli distribution with

$$\mathbb{P}(A_t = 1 \mid \bar{X}_t, \bar{A}_{t-1}, \bar{Y}_{t-1}) = \frac{e^{\gamma_1 + \gamma_X X_t + \gamma_A A_{t-1} + \gamma_Y Y_{t-1}}}{1 + e^{\gamma_1 + \gamma_X X_t + \gamma_A A_{t-1} + \gamma_Y Y_{t-1}}},$$

where $(\gamma_1, \gamma_X, \gamma_A, \gamma_Y) = (-2.5, 0, 4, 100/N)$;

3. simulate an exposure process B_t from a binomial distribution with number of trials S_{t-1} and success probability

$$p_B(\bar{A}_t, \beta) = 1 - \exp(-\eta(\bar{A}_t, \beta) I_{t-1}/N), \quad (21)$$

with $\eta(\bar{A}_t, \beta) = \exp(-\beta_0 - \beta_U U_t - \beta_X X_t - \beta_A A_t - \beta_Y Y_{t-1})$, and set $S_t = S_{t-1} - B_t$.

We considered 21 linearly spaced values of β_A in $[-1, 0]$, and for each value, we set $(\beta_0, \beta_U, \beta_X) = (1 - \beta_A/2, 0.3, 0)$ to keep η_t in the same ballpark for all values of β_A ;

4. simulate an infection process C_t from a binomial distribution with number of trials E_{t-1} and success probability $p_C = 0.2$, and set $E_t = E_{t-1} + B_t - C_t$;
5. simulate an removal process D_t from a binomial distribution with number of trials I_{t-1} and success probability $p_D = 0.2$, and set $I_t = I_{t-1} + C_t - D_t$;
6. and finally, simulate an observed time series $Y_t \equiv D_t$ for all t .

For each value of β_A , we simulated 200 time series Y_t from the SEIR model, and for each time series, we estimated $(\beta_0, \beta_X, \beta_A)$ using Method 1, assuming the SEIR model as the DGM. The other parameters were assumed to be known. Because we don't have a developed method for obtaining the MLE in this setting, we used a regressive approach. Specifically, we fitted the binomial regression model:

$$B_t \sim \text{Binomial}(S_{t-1}, \exp(-\beta_0 - \beta_X X_t - \beta_A A_t + \log(I_{t-1}/N))),$$

where $\log(I_{t-1}/N)$ is an offset. This approximates the generation of the exposure process because Eq. (21) $\approx \eta(\bar{A}_t, \beta) I_{t-1}/N$, since N is much larger than the numerator.

Fig. 6a shows the averages over the 200 simulations of the regressive estimates of β_A for each true value of β_A , along 95% confidence intervals. Phantom bias is evident.

Next we estimated (β_0, β_A) by solving the estimating equations in Eq. (14) using Method 3, assuming the SEIR model with $\eta(\bar{A}_t, \beta) = \exp(-\beta_0 - \beta_A A_t)$ as MSM, $h_t(\bar{A}_t) = (1, A_t)$, and modeling the numerator and denominator of the propensity score W_t in Eq. (13) using logistic regressions with linear AR(1) logit links, as in the previous example. Because there is no closed-form expression for $\psi(\bar{a}_t, \theta)$ or its derivative $\frac{\partial}{\partial \beta} \psi(\bar{a}_t, \theta)$, we used the Monte Carlo approximations in Eq. (15) and Example 10, and solved the estimating equations using Newton's method initialized at the regressive estimates.

Fig. 6b shows the averages over the 200 simulations of the estimating equation estimates of β_A for each true value of β_A , with 95% confidence intervals. We no longer have phantom bias.

8.3 Effect of Mobility on COVID-19 Transmission

We analyzed the effect of a mobility measure on COVID-19 death data for U.S. states, using the dataset described in Bong et al. (2024). The data are sourced from the Delphi repository at Carnegie Mellon University (delphi.cmu.edu), and consist of daily observations from February 15 to August 1, 2020 (168 days). The dataset includes state-level records of COVID-19 deaths, denoted as Y_t , and a mobility measure A_t , “proportion of full-time work”, which represents the fraction of mobile devices that spent more than six hours at a location other than their home during daytime (using SafeGraph's `full_time_work_prop`). We focused on the 30 states that reported more than 20 deaths on at least one day and truncated the time series 30 days prior to reaching a total of 10 accumulated deaths, following the procedure outlined in Bhatt et al. (2023). A preprocessing step was used to correct for the weekend effect, which shows fewer deaths reported on Saturdays and Sundays and, to compensate, more deaths reported on Mondays and Tuesdays (see Bong et al. (2024) for further details).

We modeled these data using the augmented semi-mechanistic epidemic model in Eqs. (2) and (3) and seeding mechanism described in Section 8.1. That is, we used the same DGM as in Section 8.1, except that here, we do not have covariates X_t and the treatment A_t is continuous rather than binary. Section 8.1 also contains the details for obtaining the ML estimates of (μ, β_0, β_A) and estimating equation estimates of (β_0, β_A) , although, to estimate the propensity

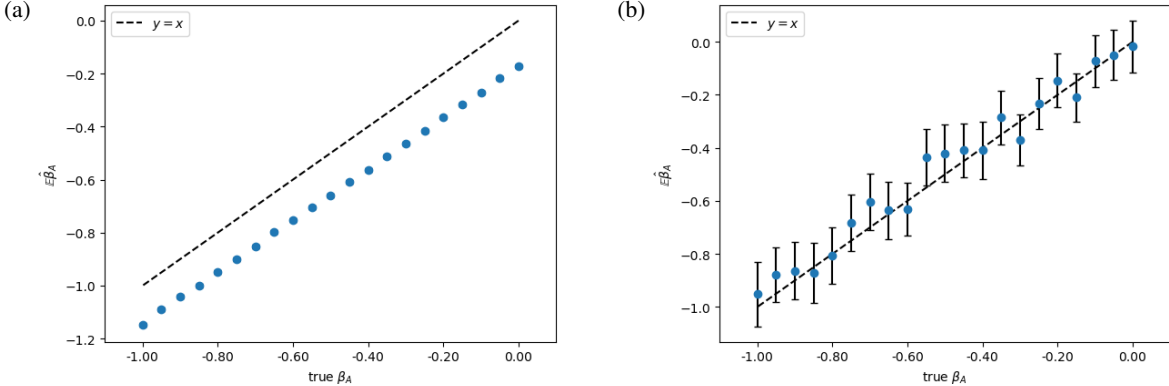


Figure 6: **Causal parameter estimation for SEIR epidemic model data.** (a) ML estimate (Method 1) and (b) estimating equation estimate (Method 3) of β_A averaged across 200 repeat simulations (blue dots) with 95%-confidence intervals, for a range of true β_A values (the errors bars are too small to be seen in (a)). There is phantom bias in (a) but not in (b).

score, we used AR(1) Gaussian regressions with identity linear links instead of logistic regressions, since the treatment is continuous.

Fig. 7a shows the estimates of β_A for the 30 states. The faint thick lines show the point estimates and 95% confidence intervals calculated separately for each state. These estimates can be improved by borrowing strength across states using a frequentist approach based on the robust empirical Bayes shrinkage method introduced by [Armstrong et al. \(2022\)](#), and extended to multivariate parameters by [Bong et al. \(2024\)](#). The dark thin estimates and intervals are the results of this procedure.

Fig. 7b shows the maximum likelihood estimates of β_A from [Bong et al. \(2024\)](#) based on the same model assumptions, and further assuming Y_t was negative binomial with mean in Eq. (2) to complete the DGM.

All estimates are positive and a few are not significantly different from zero, suggesting that reduced mobility lowered or had no significant effect on COVID-19 deaths. However, there are substantial differences between ML and estimating equation estimates. In 24 out of 30 states, the estimating equation estimates are lower than ML estimates. This result is statistically significant, assuming a binomial probability of 0.5 for the two methods yielding smaller estimates equally across all states ($p < 0.001$). This suggests the possible presence of a phantom effect, leading to ML estimates overestimating the causal effect of mobility on COVID-19 deaths.

9 Model Misspecification

To quote George E. P. Box, "All models are wrong." Consider again the example in Section 8.1. Fig. 5b illustrated that obtaining the estimate for the causal parameter β_A using estimating equations eliminated phantom bias. However, the estimate is still a little biased. This is not unexpected since the MSM we used is not consistent with the model that generated the data, that is, the MSM is misspecified. But the bias is much less than the bias of the MLE in Fig. 5a, which suffers from both misspecification bias (the likelihood we used is also misspecified since it does not include the unobserved phantoms \bar{U}_T) and phantom bias. Using Methods 2 and 4 would allow us to illustrate phantom bias without model misspecification bias in a simulation study, but they are very onerous. With Method 2, instead of assuming an MSM and deriving the causal effect $\psi(\bar{a}_t; \theta)$ from it, we would obtain $\psi(\bar{a}_t; \theta)$ by applying the g -formula in Eq. (9) to the joint distribution of $(\bar{U}_T, \bar{X}_T, \bar{A}_T, \bar{Y}_T)$ we used to simulate the data. We would need to proceed by Monte Carlo as in Eq. (15), which would be computationally very costly. With Method 4, we would construct a joint distribution P for $(\bar{U}_T, \bar{X}_T, \bar{A}_T, \bar{Y}_T)$ such that, when the g -formula is applied to P , we would get back the causal effect $\psi(\bar{a}_t; \theta)$ derived from our assumed MSM. This can be done as described in Section 7, using the construction due to [Evans and Didelez \(2024\)](#). However, doing so is quite complicated in this setting.

Notice that to proceed with Methods 2 and 4 as we just explained would require that the phantoms \bar{U}_T be modeled. This is feasible in a simulation study, but not with real data since \bar{U}_T are not observed. Therefore, in practice, all methods, including Methods 2 and 4, will suffer some degree of model misspecification. However, only Methods 2, 3 and 4 eliminate phantom bias. Method 1 does not.

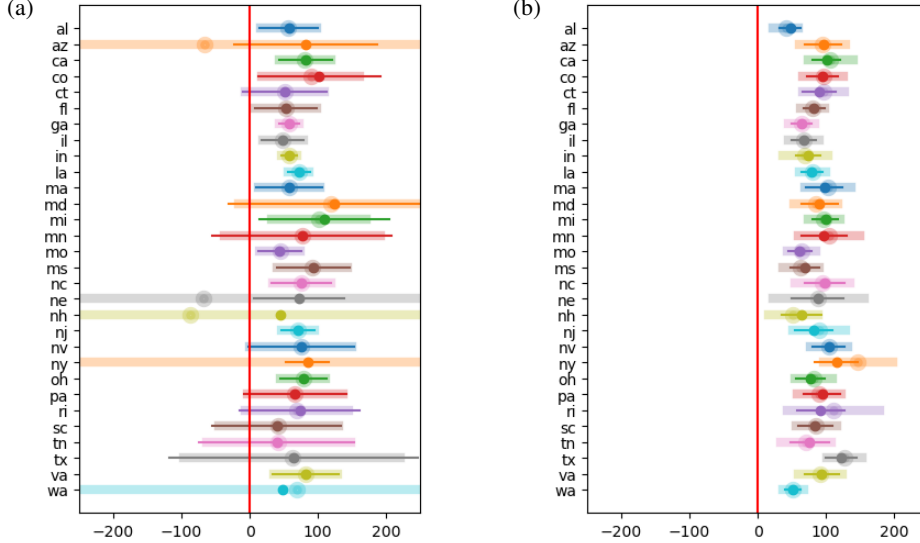


Figure 7: **Effect of a mobility measure on COVID-19 death data for 30 U.S. state, measured by β_A in Eq. (3).** Estimates and 95% confidence intervals using (a) the estimating equations in Eq. (14) (Method 3) and (b) maximum likelihood (Method 1). The faint thick lines are the estimates and intervals before shrinkage and the dark thin lines are the estimates after shrinkage.

Method	Algorithms	Specification
I	mle	joint distribution for $(\bar{X}_t, \bar{A}_t, \bar{Y}_t)$
II	estimating equations	joint distribution for $(\bar{X}_t, \bar{A}_t, \bar{Y}_t)$
III	estimating equations	MSM for $\bar{Y}_t(\bar{a}_t)$, propensity score for \bar{A}_t given the past
IV	mle	MSM for $\bar{Y}_t(\bar{a}_t)$ and copula for other variables

Table 1: *Summary of methods. In addition to the above, all the methods require the three causal assumptions (no interference, positivity and no unmeasured confounding).*

More generally, with all statistical models, there is always the danger of model misspecification. But here, the role of model misspecification is quite different for MSM's and DGM's. If a MSM is misspecified then the estimating equations at least give us an estimate of the projection of $\mathbb{E}[Y_t(\bar{a}_t)]$ onto the causal model, as discussed in [Neugebauer and van der Laan \(2007\)](#); [Martin et al. \(2024\)](#). The misspecification for DGM's is more insidious. As we have seen when discussing Method 1, essentially no sequentially parameterized DGM contains any distribution that has correlation between outcome and treatment while having no causal effect. This is a fundamental structural limitation of these models unrelated to not being able to fit the data well.

10 Conclusion

To assess the effect of interventions, one can add an intervention variable to an epidemic model. There are two interpretations of this augmented model: it is a causal model for a counterfactual or it is a data generating model for the observed variables. In the literature, these have often been treated interchangeably but, in general, these are not the same. How we estimate the parameters depends on which interpretation we use. We have discussed four approaches. See Table 1. Here we summarize the advantages and disadvantages of each.

Method 1: Use the augmented epidemic model as a data generating model, use maximum likelihood or a Bayesian approach to estimate its parameters, and then estimate the causal effect. This leads to inconsistent estimates and the *g*-null paradox. In particular, it leads to non-zero estimates of the causal effect even when there is no causal effect.

Method 2: Use the augmented epidemic model as a data generating model and apply the *g*-formula to that DGM to extract the causal model. Also use the DGM to derive the propensity score. Then use estimating equations to estimate the parameters. This avoids the *g*-null paradox but the method is quite cumbersome and the causal model is not easily interpretable. An additional problem is that we have to divide by the propensity score, which can cause the parameter estimates to have large variances if the propensity score gets small.

Method 3: Use the augmented epidemic model as a marginal structural model. Postulate a model for the propensity score. Then use estimating equations to estimate the model parameters. This is the simplest approach, and because it treats the augmented epidemic model as a model of how the intervention affects the outcome, it facilitates the interpretation of treatment on outcome. But like Method 2, we have to divide by the propensity score, so parameter estimates can have large variances.

Method 4: Use the augmented epidemic model as a marginal structural model. Construct a model for the data generating process that is consistent with the marginal structural model, and then use maximum likelihood to estimate the model parameters. The advantages of this method are that it avoids the g -null paradox and dividing by the propensity score. The disadvantages are that it is complicated and requires more modeling assumptions. The method also requires more investigation.

Methods 2, 3 and 4 avoid phantom bias. If we have a good understanding of the full data generating process, then building a DGM for Method 2 may offer a more principled and realistic generative perspective. But Method 2 does not allow one to specify a model for the treatment effect. Rather, the treatment effect is implied by the g -formula, will not typically be available in closed form and will not be easily interpretable. Method 3 does not need the full DGM but still requires a model for the propensity score, so at least part of what we understand about the data generating process can be incorporated there. But unlike Method 2, Method 3 allows us to specify an interpretable causal model for the treatment effect. In Method 4, as in Method 3, we explicitly state the model for the effect of treatment, and we then build a full DGM around that specification. So Method 4 is interpretable and arguably more principled than Method 3. However, Method 4 is quite new and there is not yet a lot of experience that would inform the practical aspects of implementing it especially in the case of a single time series. In particular, constructing and estimating the copula model is non-trivial. So Method 4 seems promising from the aspect of interpretability and in terms of avoiding phantom bias but more work is needed to see how practical it is.

Whichever approach one uses, it is important to distinguish causal models and data generating models. And, when estimating parameters, it is important to account for confounding. No matter how many confounders we include in an analysis, there is always the danger that there are important unobserved confounders. There are some methods for dealing with unobserved confounding. One of the oldest is to include instrumental variables which are variables that affect intervention but do not directly affect the outcome (Greenland, 2000). More recently, there has been a surge of interest in using negative controls, which are variables unaffected by intervention, as a way to control for unobserved confounding (Tchetgen Tchetgen et al., 2024). We will report on these methods as applied to epidemic modeling in future work.

Although completely nonparametric inference is not possible for a single time series, a referee suggested that using a partially nonparametric data generating model might reduce phantom bias and misspecification bias and might still be estimable. This is a reasonable suggestion that deserves investigation.

Finally, let us mention that another interesting direction would be to develop structural nested models (SNM) (Vansteelandt et al., 2014; Robins, 2000) for epidemics. These models allow one to model effect modification using models for counterfactual contrasts that include covariates. An example of a structural nested model in a simple setting is

$$\mathbb{E}[Y(a)|X = x, A = a] - \mathbb{E}[Y(0)|X = x, A = a] = a(\psi_0 + \psi_1 x).$$

The causal parameter ψ can be estimated using appropriate estimating equations. These models also exist for time varying setting. Building SNM's that somehow incorporate epidemic models is an open problem that deserves further investigation.

References

Ackley, S. F., Mayeda, E. R., Worden, L., Enanoria, W. T., Glymour, M. M., and Porco, T. C. (2017). Compartmental model diagrams as causal representations in relation to DAGs. *Epidemiologic methods*, 6(1):2016007.

Andrews, D. W. (1988). Laws of large numbers for dependent non-identically distributed random variables. *Econometric theory*, 4(3):458–467.

Andrews, D. W. (1991). An empirical process central limit theorem for dependent non-identically distributed random variables. *Journal of Multivariate Analysis*, 38(2):187–203.

Armstrong, T. B., Kolesár, M., and Plagborg-Møller, M. (2022). Robust empirical bayes confidence intervals. *Econometrica*, 90(6):2567–2602.

Babino, L., Rotnitzky, A., and Robins, J. (2019). Multiple robust estimation of marginal structural mean models for unconstrained outcomes. *Biometrics*, 75(1):90–99.

Barrero Guevara, L. A., Kramer, S. C., Kurth, T., and Domenech de Cellès, M. (2025). Causal inference concepts can guide research into the effects of climate on infectious diseases. *Nature Ecology & Evolution*, 9(2):349–363.

Bates, S., Kennedy, E., Tibshirani, R., Ventura, V., and Wasserman, L. (2022). Causal inference with orthogonalized regression: Taming the phantom. *arXiv preprint arXiv:2201.13451*.

Bhatt, S., Ferguson, N., Flaxman, S., Gandy, A., Mishra, S., and Scott, J. A. (2023). Semi-mechanistic bayesian modelling of COVID-19 with renewal processes. *Journal of the Royal Statistical Society Series A: Statistics in Society*, 186(4):601–615.

Bong, H., Ventura, V., and Wasserman, L. (2024). Frequentist inference for semi-mechanistic epidemic models with interventions. *Journal of the Royal Statistical Society Series B: Statistical Methodology*, page qkae110.

Bonvini, M., Kennedy, E., Ventura, V., and Wasserman, L. (2021). Causal inference in the time of Covid-19. *arXiv preprint arXiv:2103.04472*.

Bonvini, M., Kennedy, E. H., Ventura, V., and Wasserman, L. (2022). Causal inference for the effect of mobility on COVID-19 deaths. *The Annals of Applied Statistics*, 16(4):2458–2480.

Cai, X., Zeng, L., Fowler, C., Dixon, L., Ongur, D., Baker, J. T., Onnela, J.-P., and Valeri, L. (2024). Causal estimands and identification of time-varying effects in non-stationary time series from n-of-1 mobile device data. *arXiv preprint arXiv:2407.17666*.

Callaway, B. and Li, T. (2023). Policy evaluation during a pandemic. *Journal of Econometrics*, 236(1):105454.

Chernozhukov, V., Kasahara, H., and Schrimpf, P. (2020). Causal impact of masks, policies, behavior on early covid-19 pandemic in the us. *Journal of econometrics*, 220(1):23.

De Jong, R. M. (1997). Central limit theorems for dependent heterogeneous random variables. *Econometric Theory*, 13(3):353–367.

De Jong, R. M. and Davidson, J. (2000). Consistency of kernel estimators of heteroscedastic and autocorrelated covariance matrices. *Econometrica*, 68(2):407–423.

Evans, R. J. and Didelez, V. (2024). Parameterizing and simulating from causal models. *Journal of the Royal Statistical Society Series B: Statistical Methodology*, 86(3):535–568.

Feller, A. and Gelman, A. (2015). Hierarchical models for causal effects. *Emerging trends in the social and behavioral sciences*, 1:16.

Feng, S. and Bilinski, A. (2024). Parallel trends in an unparalleled pandemic: Difference-in-differences for infectious disease policy evaluation. *medRxiv*, pages 2024–04.

Flaxman, S., Mishra, S., Gandy, A., Unwin, H. J. T., Mellan, T. A., Coupland, H., Whittaker, C., Zhu, H., Berah, T., Eaton, J. W., et al. (2020). Estimating the effects of non-pharmaceutical interventions on covid-19 in europe. *Nature*, 584(7820):257–261.

Gibson, G. J. and Renshaw, E. (1998). Estimating parameters in stochastic compartmental models using Markov chain methods. *Mathematical Medicine and Biology: A Journal of the IMA*, 15(1):19–40.

Giffin, A., Gong, W., Majumder, S., Rappold, A. G., Reich, B. J., and Yang, S. (2022). Estimating intervention effects on infectious disease control: The effect of community mobility reduction on coronavirus spread. *Spatial Statistics*, 52:100711.

Greenland, S. (2000). An introduction to instrumental variables for epidemiologists. *International journal of epidemiology*, 29(4):722–729.

Grigorieva, E. V. and Khailov, E. N. (2015). Optimal intervention strategies for a seir control model of ebola epidemics. *Mathematics*, 3(4):961–983.

Halloran, M. E. and Struchiner, C. J. (1995). Causal inference in infectious diseases. *Epidemiology*, 6(2):142–151.

Hernan, M. and Robins, J. (2020). *Causal Inference: What If*. Chapman & Hall/CRC.

Imbens, G. W. and Rubin, D. B. (2015). *Causal inference in statistics, social, and biomedical sciences*. Cambridge university press.

Joe, H. (2014). *Dependence modeling with copulas*. CRC press.

Kennedy, E. H., Joffe, M. M., and Small, D. S. (2015). Optimal restricted estimation for more efficient longitudinal causal inference. *Statistics & probability letters*, 97:185–191.

Kermack, W. O. and McKendrick, A. G. (1927). A contribution to the mathematical theory of epidemics. *Proceedings of the royal society of london. Series A, Containing papers of a mathematical and physical character*, 115(772):700–721.

Lekone, P. E. and Finkenstädt, B. F. (2006). Statistical inference in a stochastic epidemic seir model with control intervention: Ebola as a case study. *Biometrics*, 62(4):1170–1177.

Lin, X., Manela, D. d. V., Mathis, C., Tarp, J. M., and Evans, R. J. (2025). Exact simulation of longitudinal data from marginal structural models. *arXiv preprint arXiv:2502.07991*.

Martin, A., Santacatterina, M., and Díaz, I. (2024). Non-parametric efficient estimation of marginal structural models with multi-valued time-varying treatments. *arXiv preprint arXiv:2409.18782*.

Mode, C. J. and Sleeman, C. K. (2000). *Stochastic processes in epidemiology: HIV/AIDS, other infectious diseases and computers*. World Scientific.

Neugebauer, R. and van der Laan, M. (2007). Nonparametric causal effects based on marginal structural models. *Journal of Statistical Planning and Inference*, 137(2):419–434.

Newey, W. K., West, K. D., et al. (1987). A simple, positive semi-definite, heteroskedasticity and autocorrelation consistent covariance matrix. *Econometrica*, 55(3):703–708.

N'konzi, J.-P. N., Chukwu, C. W., and Nyabadza, F. (2022). Effect of time-varying adherence to non-pharmaceutical interventions on the occurrence of multiple epidemic waves: A modeling study. *Frontiers in Public Health*, 10:1087683.

Pan, W. and Bai, H. (2018). Propensity score methods for causal inference: an overview. *Behaviormetrika*, 45(2):317–334.

Pearl, J. (2009). *Causality*. Cambridge university press.

Robins, J. M. (1986). A new approach to causal inference in mortality studies with a sustained exposure period—application to control of the healthy worker survivor effect. *Mathematical Modelling*, 7(9):1393–1512.

Robins, J. M. (2000). Marginal structural models versus structural nested models as tools for causal inference. In Halloran, M. E. and Berry, D., editors, *Statistical Models in Epidemiology, the Environment, and Clinical Trials*, pages 95–133, New York, NY. Springer New York.

Robins, J. M., Hernán, M. A., and Brumback, B. (2000). Marginal structural models and causal inference in epidemiology. *Epidemiology*, 11(5):550–560.

Robins, J. M. and Wasserman, L. (1997). Estimation of effects of sequential treatments by reparameterizing directed acyclic graphs. In *Proceedings of the Thirteenth Conference on Uncertainty in Artificial Intelligence*, UAI'97, page 409–420, San Francisco, CA, USA. Morgan Kaufmann Publishers Inc.

Tchetgen Tchetgen, E. J., Ying, A., Cui, Y., Shi, X., and Miao, W. (2024). An introduction to proximal causal inference. *Statistical Science*, 39(3):375–390.

Tomaselli, L., Ventura, V., and Wasserman, L. (2025). Robust simulation based inference. *arXiv preprint arXiv:2508.02404*.

Vansteelandt, S., Joffe, M., et al. (2014). Structural nested models and g-estimation: the partially realized promise. *Statistical Science*, 29(4):707–731.

Weinstein, E. N. and Blei, D. M. (2024). Hierarchical causal models. *arXiv preprint arXiv:2401.05330*.

Zhou, X. and Wodtke, G. T. (2020). Residual balancing: A method of constructing weights for marginal structural models. *Political Analysis*, 28(4):487–506.

A Appendix

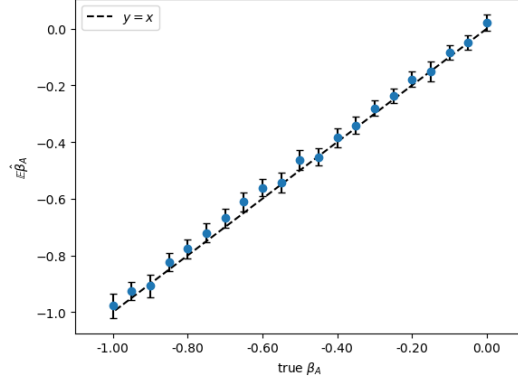


Figure A.1: **Point estimates (blue dots) and 95%-confidence intervals (error bars) of β_A from the ML estimates without phantom variables.** For each true β_A value, the point estimate and confidence interval were obtained from 200 i.i.d. estimates $\hat{\beta}_A$. The ML estimates are unbiased when phantom variables are absent.